



Cite this: *J. Mater. Chem. B*, 2015,
3, 7125

Antibacterial and photochemical properties of cellulose nanofiber–titania nanocomposites loaded with two different types of antibiotic medicines†

O. L. Galkina,^{ab} K. Önneby,^b P. Huang,^c V. K. Ivanov,^{de} A. V. Agafonov,^{ae}
G. A. Seisenbaeva^{bf} and V. G. Kessler^{*bf}

Nanocomposite dermal drug delivery systems based on cellulose nanofibers with grafted titania nanoparticles loaded by two antibiotic medicines from different classes, *i.e.* tetracycline (TC) and phosphomycin (Phos), were successfully produced by a “green chemistry” approach in aqueous media. The influence of a different surface binding mechanism between the drug molecule and modified cellulose nanofibers on the release of the drug and, as a result, on antimicrobial properties against common pathogens Gram-positive, *Staphylococcus aureus* and Gram-negative *Escherichia coli* was investigated. The disk diffusion method and broth culture tests using varying concentrations of drugs loaded to nanocomposites were carried out to investigate the antibacterial effects. The influence of UV irradiation on the stability of the obtained nanocomposites and their antibacterial properties after irradiation were also investigated, showing enhanced stability especially for the TC loaded materials. These findings suggest that the obtained nanocomposites are promising materials for the development of potentially useful antimicrobial patches.

Received 10th July 2015,
Accepted 6th August 2015

DOI: 10.1039/c5tb01382h

www.rsc.org/MaterialsB

Introduction

During the last few decades the interest in development of controlled drug delivery approaches has been constantly growing, covering practically all types of ordination, such as oral,¹ parenteral,² submucosal³ or pulmonary⁴ ones. In recent years, the increasing resistance of microorganisms against antibiotics in the treatment of wounds has led to the renaissance of antiseptic drugs for local application in the prophylaxis and treatment of wound infections,⁵ permitting potentially to decrease the release of non-destroyed drugs into wastewaters, inevitable otherwise in per-oral ordination. Transdermal and dermal drug delivery is one of the promising alternative methods for controlled release through skin.^{6,7}

The most advantageous features of these patches include local, controlled antibiotics release with dose above the bacteria's minimum inhibitory concentration for protection and treatment against infection.^{8,9} Furthermore, physical and chemical properties of dermal patches permit us to use relatively strong medicines with a high molecular weight as well as poorly water soluble drugs but with minimal risk of toxicity.¹⁰

Potential application of a nanotechnology-based system in the biomedical field attracted the interest of many research groups worldwide.¹¹ Cellulose and its derivatives in various types of formulations have a long history in the pharmaceutical industry.¹² Due to unique specific properties, the use of nanoscaled cellulose as a novel biomedical material for drug delivery application is the most interesting and addressed topic for biologists and material scientists, but many issues are still not clearly investigated, especially interactions between drug molecules and nanocellulose,¹³ chemical binding for controlled drug release,^{14,15} possible reduction or loss of drug activity.¹⁶ In a recent study, wound dressing based on bacterial nanocellulose loaded with the antiseptic octenidine was developed as drug a delivery system for the treatment of acute and chronically infected wounds.⁵

To the best of our knowledge, our recent work was the first in which nanocomposites with potential for dermal drug delivery were developed, using nanotitania chemically grafted onto nanocellulose as an active ingredient for enhanced uptake and controlled release of model drug loads.¹⁷ The aim of the

^a G.A. Krestov Institute of Solution Chemistry of the Russian Academy of Sciences, Akademicheskaya St., 1, Ivanovo, Russia. E-mail: olga.galkina@slu.se, ava@isc-ras.ru

^b Department of Chemistry and Biotechnology, Swedish University of Agricultural Sciences, 750 07 Uppsala, Sweden. E-mail: vadim.kessler@slu.se, gulaim.seisenbaeva@slu.se, Karin.Onneby@slu.se

^c Molecular Biomimetics, Department of Chemistry – Ångström, Uppsala University, Box 523, SE 751 20, Uppsala, Sweden

^d Kurnakov Institute of General and Inorganic Chemistry, Leninskiipros. 31, Moscow, Russia. E-mail: van@igic.ras.ru

^e National Research Tomsk State University, 36 Lenin Av., Tomsk, 634050, Russia

^f CaptiGel AB, Virdings allé 32B, 75450 Uppsala, Sweden

† Electronic supplementary information (ESI) available. See DOI: 10.1039/c5tb01382h

present work was to bring insight into how the chemical binding of the two chemically different drugs, tetracycline (TC) and phosphomycin (Phos), to the carrier is influencing the antimicrobial efficacy of nanocomposites based on cellulose nanofibers and grafted titania. The viability on the action of the released drug was examined for two common potential pathogen microorganisms: *Staphylococcus aureus* and *Escherichia coli*.

Experimental

Sulphuric acid (H_2SO_4 , 98 wt%), 1,2,3,4-butanetetracarboxylic acid (BTCA), sodium hypophosphite (NaH_2PO_2), tetracycline ($\text{C}_{22}\text{H}_{24}\text{N}_2\text{O}_8 \cdot \text{xH}_2\text{O}$, $M_w \sim 444.43$), phosphomycin disodium salt ($\text{C}_3\text{H}_5\text{Na}_2\text{O}_4\text{P}$, $M_w \sim 182.02$), polyvinyl alcohol (PVA, M_w 146 000–186 000) were purchased from Sigma-Aldrich. The TiO_2 nanosol was produced by CaptiGel AB, Uppsala, Sweden. Raw cotton (100%) was used as a starting material.

Synthetic procedures

Preparation of cellulose nanofibers. The detailed synthesis procedure of cellulose nanofibers–titania nanocomposites has been recently described by us elsewhere.¹⁷ Briefly, for obtaining cellulose nanofibers we have developed a method using a copper ammonium complex for converting raw cotton into a molecular solution with subsequent regeneration of cellulose by acid hydrolysis. Firstly, raw cotton was completely dissolved in Schweitzer's reagent (tetrammindiaquacopper(II) hydroxide). Then 25 mL of Schweitzer's reagent solution, containing the dissolved cotton, were added into 140 mL of the sulphuric acid solution (40 wt%) and stirred vigorously at 60 °C for 4 hours. After that, hydrolysis was immediately quenched by adding 500 mL of cold water to the reaction mixture. The resulting suspension was separated from sulphuric acid by several cycles of centrifuging and washing with distilled water until pH = 6.

Preparation of nanocomposites loaded with the model drugs. Firstly, to cross-link titania nanoparticles with cellulose nanofibers, 1,2,3,4-butanetetracarboxylic acid (BTCA) was used as a spacer in the presence of sodium hypophosphite (SHP) as a catalyst. The obtained aqueous suspensions of cellulose nanofibers were thus treated by BTCA (0.002 mol) with SHP (0.002 mol) aqueous solution at 70 °C for 2 h. The BTCA-treated cellulose nanofibers were modified by TiO_2 nanosol and drug by using three different methods.

Method #0 (M0). The drug powder (TC or Phos) was initially dissolved in water, and then added to an aqueous suspension of cellulose nanofibers. The mixture was kept at 40 °C and 70 °C

for 2 h for TC and Phos, respectively. The obtained nanocomposites were dried at 40 °C for 48 h.

Method #1 (M1). TC drug powder was initially dissolved in titania nanosol and thereafter the obtained solution was added to an aqueous suspension of cellulose nanofibers and kept at 40 °C for 2 h. The obtained nanocomposites were dried at 40 °C for 48 h.

Method #2 (M2). The Phos powder was initially dissolved in water and then added together with the titania nanosol simultaneously to an aqueous suspension of cellulose nanofibers. The mixture was kept at 70 °C for 2 h. The obtained nanocomposites were dried at 40 °C for 48 h.

The composition of the obtained samples and the method of drug modification are presented in the Table 1. In order to obtain nanocomposites as a film, 3% of the PVA additive was used.

Characterization

IR spectra of all samples were obtained using a Perkin Elmer FT-IR spectrometer Spectrum-100. A total of 8 scans were carried out on wavenumbers from 400 cm^{-1} to 4000 cm^{-1} , in transmittance mode. All spectra were smoothed and baseline corrected.

In vitro drug release

To investigate the release profile of TC, the nanocomposites containing TiO_2 and TC were incubated in 300 mL of citrate buffer (0.02 M, pH = 6) at constant temperature (37 ± 0.5 °C) upon constant stirring at 100 rpm. At determined time intervals, 1 mL of each solution was taken out for analysis, and the same volume of fresh medium was added to maintain a constant volume. TC content in each aliquot was determined by spectrophotometry. UV-Vis quantitative analysis of drugs was performed on a UV/Vis spectrophotometer UV-1800. A linear calibration curve for TC was obtained at 375 nm. Released drug was determined by using the following equation:

$$\text{Drug release (\%)} = (\text{released drug})/(\text{total drug}) \times 100$$

where released drug was calculated from the drug concentration measured in the total volume and total drug was the amount loaded in the obtained sample.

Photocatalytic activity determination

Photocatalytic activity of pure cellulose nanofibers and nanocomposites was tested by the rate of decomposition of Rhodamine B under the influence of UV irradiation. The source of UV radiation was a high-pressure 250 W mercury lamp with radiation maximum at 365 nm. The prepared samples had a diameter of 9 cm. Then 2 mL of Rhodamine B solution (0.04 g L^{-1}) was added to the samples. The colored samples were dried and subjected to UV

Table 1 Composition of the samples

| Sample | BTCA (mol) | SHP (mol) | TiO_2 (mol) | Drug (mol) | Method of modification |
|------------------------------|------------|-----------|----------------------|-----------------------|------------------------|
| CNF_ TiO_2 | 0.002 | 0.002 | 1.5×10^{-4} | — | — |
| CNF_TC_M0 | — | — | — | 4.74×10^{-5} | Method #0 |
| CNF_Phos_M0 | — | — | — | 4.74×10^{-5} | Method #0 |
| CNF_ TiO_2 _TC_M1 | 0.002 | 0.002 | 1.5×10^{-4} | 4.74×10^{-5} | Method #1 |
| CNF_ TiO_2 _Phos_M2 | 0.002 | 0.002 | 1.5×10^{-4} | 4.74×10^{-5} | Method #2 |

irradiation for 30 min. Difference in color for each sample before and after UV irradiation is the corresponding factor for the determination of TiO_2 photocatalytic effects on the decomposition of dye stains.

For kinetic studies the dry discs were immersed into the Rhodamine B stock solution (80 mL) and subjected to UV irradiation for given periods of time (up to 30 min when the total discoloration occurred). The temperature of the reaction solution was held at 25 ± 0.5 °C. The changes in the dye concentrations were determined using a PG Instruments T70 + UV/VIS spectrophotometer at the adsorption maximum at $\lambda = 554 \text{ cm}^{-1}$.

Electron paramagnetic resonance

X-band EPR measurements were performed on a Bruker ELEXYS E500 spectrometer equipped with a SuperX EPR049 microwave bridge and a cylindrical TE_{011} ER 4122SHQE cavity. Temperature was controlled using an Oxford Instruments ESR 900 flow cryostat. The EPR sample prepared as wet gels without drying (CNFs with Phos) is denoted as PCNFs (*i.e.* CNF_ TiO_2 _Phos_M2); parallel samples were either UV irradiation for 5 min denoted as PH_irr or UV-irradiated and kept for 5 days as PH5d_irr. After preparation the samples were transferred to EPR tubes and immediately frozen in a liquid nitrogen bath. Before EPR examination all samples were also Ar gas flushed.

In vitro antibacterial studies

Minimum inhibitory concentration. Minimum inhibitory concentration (MIC) was determined for pure drugs by broth micro dilution using Mueller-Hinton (MH) broth (OXOID, England) loaded with TC ($0.5\text{--}100 \mu\text{g mL}^{-1}$) or Phos ($1\text{--}200 \mu\text{g mL}^{-1}$). McFarland 0.5 dilutions from overnight cultures of the Gram-positive bacteria *Staphylococcus aureus* strain NBRC 100910 and the Gram-negative *Escherichia coli* strain NCTC9001 were used as inoculum. After 18 h of incubation at 37 °C the MIC was defined as the lowest concentration of antibiotic with no visible growth and by viable count (VC). VC was determined by 10-fold serially dilutions plated on MH agar (OXOID, England) and incubated at 37 °C overnight. Colonies were counted and colony forming units (CFU) per mL were calculated.

Disk diffusion method for antibacterial activity. The disk diffusion method (EUCAST, 2014)¹⁸ was used to assay the antibacterial activity of the cellulose nanofibers and nanocomposites loaded with TC or Phos ($1\text{--}100 \mu\text{g}$ per disk) against test strains *S. aureus* and *E. coli* on MH agar plates. Pure cellulose nanofibers and nanocomposites with TiO_2 were used as controls. Inhibition zone diameters were measured after incubation at 37 °C for 18 h. Experiments were performed with biological triplicate. In addition, bacterial susceptibility testing was carried out on CNF_TC_M0 and CNF_ TiO_2 _TC_M1 samples with $1\text{--}100 \mu\text{g}$ of TC after UV-irradiation for 30 and 60 min, using a high-pressure 250 W mercury lamp with radiation maximum at 365 nm.

Liquid broth assay for antibacterial activity testing. Long-term release of TC and Phos loaded to cellulose nanofibers and nanocomposites was studied in a liquid broth assay. CNF_TC_M0, CNF_ TiO_2 _TC_M1 samples with $1\text{--}10 \mu\text{g mL}^{-1}$ of TC and

CNF_Phos_M0, CNF_ TiO_2 _Phos_M2 samples with $100 \mu\text{g mL}^{-1}$ of Phos were added to MH broth 0, 12, 18 and 24 h before inoculation with 0.5 McFarland of *S. aureus*. After 18 h of incubation at 37 °C the growth inhibiting effect was determined by VC and expressed as % in relation to CFU of the control without addition of CNFs. To simulate body fluid conditions, citrate buffer (0.75 mL , 0.03 M , $\text{pH} = 6$) was added to MH broth. Experiments were performed with biological triplicate.

Results and discussion

I. Characterization of TiO_2 -nanocellulose nanocomposites loaded with different drugs

In our previous study,¹⁷ we discussed the drug delivery matrices employing nanotitania as an active component for the drug binding and retention. It turned crucial to chemically bind titanium dioxide to nano cellulose using the butane tetracarboxylic acid linker (BTCA) in order to ensure the retention of titania within the material. BTCA is acting as a linker, being connected to cellulose *via* ester bonds and to titania - *via* surface complexation with the carboxylate moieties. Both types of bonds are easily distinguishable with FTIR, please see ref. 17 and below for details. Esterification of cellulose with carboxylic acids is not straightforward in aqueous medium and requires application of nucleophilic catalysts, for example, sodium hypophosphate (SHP) used in this work. The use of SHP for this purpose is a well established procedure and the mechanism of its action and removal on washing have been described in detail in the literature.^{19,20} The applied nano cellulose consists of small globules just a few dozen nm in size. Grafting of small TiO_2 nanoparticles (3.5 nm in size) does not change the overall morphology of the material (see Fig. 1 and discussion below).

The obtained results showed that using different types of drug modification can lead to various interactions between TiO_2 and drug molecules resulting in different kinetics of drug release. In this study, we strive to gain knowledge on the influence of different types of drugs and thus different interactions between drugs and CNFs on antimicrobial activity of the obtained nanocomposites. For this purpose, two antibiotic drugs from different classes, namely TC and Phos, were chosen as model drugs for modification of cellulose nanofibers and further investigation of their antibacterial properties. Phos is binding to titania *via* complexation with the surface cations through phosphonate function, offering the formation of highly dissociation-stable complexes.²¹ Release of phosphonate-anchored molecules from TiO_2 nanostructures was identified as a 1st order reaction completed within weeks.²² Phos [(2*R*,3*S*-3-methyloxiran-2-yl)-phosphonic acid] is a natural broad spectrum antibiotic compound which is mainly used for the treatment of uncomplicated urinary tract infections and meningitis, pneumonia, and pyelonephritis.²³ TC is supposedly binding to the titania surface through the formation of phenoxide complexes, which are also considered as quite stable.²⁴ Application of a catecholate function has even been proposed as an alternative to phosphate or phosphonate in stable grafting of ligands onto metal oxides.²⁵ TC was selected

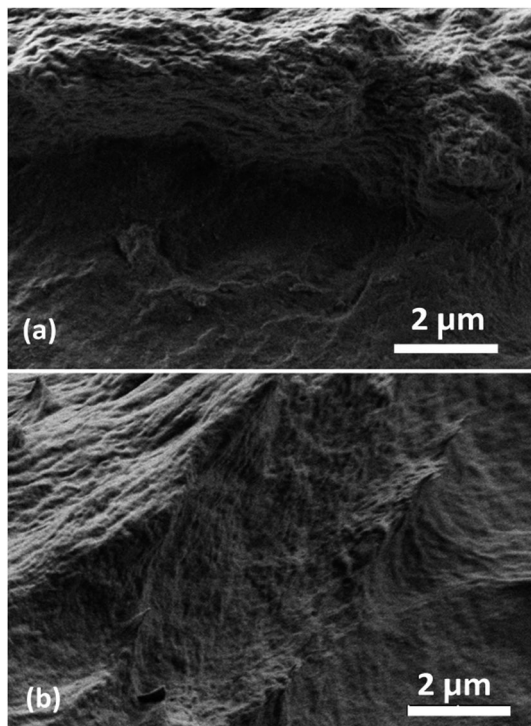


Fig. 1 SEM images of the applied nanomaterials: (a) PCNFs, (b) CNF₂TiO₂.

also, on the other hand, because of its broad application as antibiotic in the treatment of skin bacterial infections, arising from its antimicrobial activity against numerous medically relevant aerobic and anaerobic bacterial genera, both Gram-positive and Gram-negative.²⁶ Moreover, TC was included in the World Health Organization's List of Essential Medicines as one of the most important medications needed in a basic health system.²⁷ Drug modification of nanocomposites was performed by three different methods, which are described in the experimental part and named M0, M1, and M2. Drug grafting was performed in amounts calculated in assumption of the formation of a uniform, single layer coverage on a TiO₂-modified cellulose nanofiber surface²¹ (see ESI† for explanation). As in our previous investigation,¹⁷ method #2 was chosen for Phos, which otherwise (produced *via* M#1) prevents titania from binding to nanocellulose. TC was incorporated into nanocomposites using methods #1. Thus, total amounts of TC and Phos in the obtained nanocomposites were 4.6 wt% and 4.7 wt%, respectively, introduced as weighted amounts of solid drugs.

To provide insight into the possible interaction between drugs and nanocomposites, the FT-IR spectra of PCNFs, CNF₂TiO₂, CNF₂TiO₂-TC-M1 samples are shown in Fig. 2. No new absorption peaks after Phos modification were observed for CNF₂TiO₂-Phos-M2¹⁷ (see also Fig. S1, ESI†). For this reason, we confirmed the formation of a chelating complex between titania and drug molecules by UV-Vis spectroscopy (please, see Fig. S2, ESI†). The spectrum revealed a well-defined maximum at 310 nm – a distinct shift to shorter wavelengths compared to the derivatives of carboxylic acids (375 nm for the surface complex with Diclophenac and 474 nm for that with

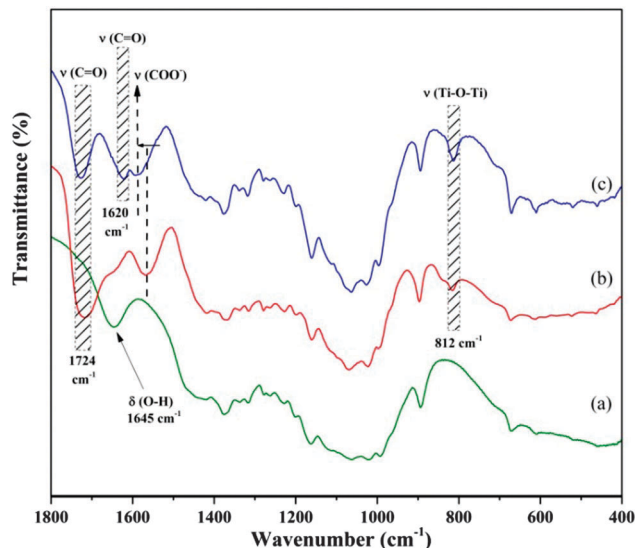


Fig. 2 FTIR spectra of PCNFs (a), CNF₂TiO₂ (b) and CNF₂TiO₂-TC-M1 (c).

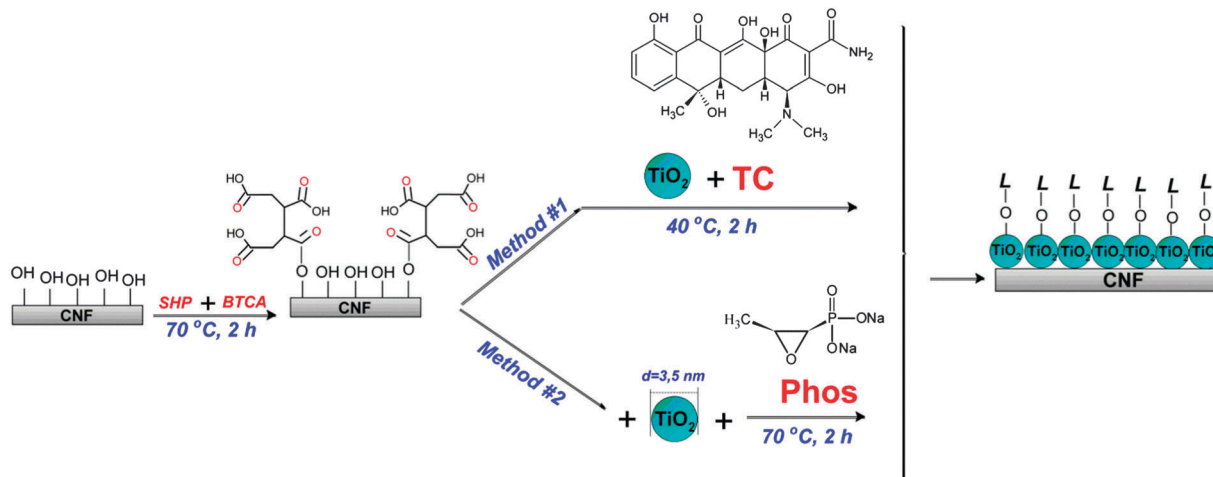
the D Penicillamine),¹⁷ indicating relatively stronger bonding to the phosphonate ligand.

As mentioned above, TiO₂ was used as a binding agent between cellulose nanofibers and the drug molecule. Compared to the starting material (PCNFs), the presence of adsorption peaks in the 1800–1600 cm⁻¹ region confirmed the binding of TiO₂ nanoparticles with cellulose nanofibers *via* formation of transverse ester bonds under the action of the cross-linking agent 1,2,3,4-butanetetracarboxylic acid in the obtained samples (see Scheme 1).²⁸ Particularly, the absorption peaks at 1565 cm⁻¹ and 1724 cm⁻¹ are assigned to stretching vibrations of COO⁻ and C=O functional groups in the CNF₂TiO₂ sample.

The weak absorption peaks at 812 cm⁻¹ are attributed to Ti–O–Ti vibration. The absorption peak at 1642 cm⁻¹ indicates the presence of water. The CNF₂TiO₂-TC-M1 sample has shown all the above characteristic peaks but with a slight shift of COO⁻ stretching vibration to higher wavelengths (from 1565 cm⁻¹ to 1576 cm⁻¹). This shifting can be attributed to the formation of new bonds between TC and the nanocomposite through phenoxide groups. At the same time, the presence of a drug in the samples could also be confirmed by the appearance of a new absorption peak at 1620 cm⁻¹ corresponding to the stretching vibration of C=O aromatic ring carbonyl groups in TC.²⁹

***In vitro* drug release.** In our previous investigation,¹⁷ we already determined the *in vitro* kinetics of Phos release from nanocomposites based on cellulose nanofibers and TiO₂, performing radio-labeling analysis of a ³³P-marked phosphorylated model drug (ATP). In particular, the release of ³³P-marked ATP from the CNF₂TiO₂ sample occurred in two steps: firstly, 40% of ³³P-marked ATP dissociated after the first 4 h and only an additional 25% dissociated in the following 100 h. The obtained results showed very long-term release for the strongly chemisorbed medicine.

In this work, we report the studies of drug release of TC incorporated into cellulose nanofibers by two different methods.



Scheme 1 Preparation of nanocomposites based on cellulose nanofibers and titania grafted with two types of drugs (TC and Phos – L) by two different methods: M1, M2 – method #1 and #2, respectively. SHP – sodium hypophosphite; BTCA – 1,2,3,4-butanetetracarboxylic acid.

The *in vitro* release profile of TC from CNF_TC_M0 and CNF_TiO₂_TC_M1 samples is shown in Fig. 3. According to the obtained results, without using titania as a binding agent, TC had a burst release from the CNF_TC_M0 sample of 37% in the first two minutes. In fact, about 80% of the total drug was released after 4 hours.

In this case, the burst release profile of TC can be explained by physical adsorption of the drug onto the cellulose nanofiber surface. In contrast, the CNF_TiO₂_TC_M1 sample displayed a sustained long-term release profile of TC where around 80% of the drug was released in a controlled manner over 7 hours without any initial burst effect.

So, these studies clearly demonstrated that application of titania as a binding agent between drug molecules and the biopolymer matrix provided a sustained long-term release.

It should also be mentioned that antibiotic formulations are usually applied topically three or four times a day in order to achieve the recommended dosage.^{30,31} In comparison with

them, the benefits on the use of the developed nanocomposites as antibiotic patches with ability of sustained drug release offer an enhancement of local concentration of the antibiotics without necessity of frequent dressing changes. Thus, the nanocomposites produced by this technology have promising performance as wound-dressing materials and, as shown recently, even as anesthetics and analgesics.¹⁷

II. Antibacterial activity of cellulose nanofibers–titania nanocomposites loaded with two different drugs

The aim of the biological susceptibility tests was to get an insight into how the discovered different release kinetics could influence the antibacterial effects of the drugs after release. The biological activity of TC and Phos released from the obtained samples was thus investigated by disk diffusion and broth culture assays against two bacterial strains, *S. aureus* and *E. coli*, representing a potential Gram-positive and Gram-negative pathogen.

The minimal inhibitory concentration (MIC) against the two strains differs for TC and Phos. To be able to directly compare the antibacterial effect of the cellulose nanofibers loaded with the two drugs, their MIC-values have to be taken into account. TC showed higher activity against the *S. aureus* strain with an MIC-value of 1 µg mL⁻¹ compared to the *E. coli* strain of 5 µg mL⁻¹. Phos exhibited a MIC-value of 10 µg mL⁻¹ against *S. aureus* and >100 µg mL⁻¹ for *E. coli*. The results of the disk diffusion tests are shown in Fig. 4, 5 and in Table S1 (please, see ESI[†]). Neither pure cellulose nanofibers nor cellulose nanofibers modified only with titania showed any antibacterial activity for either of the bacteria strains. This is in accordance with our earlier studies using biocompatible titania nanoparticles as bio-encapsulation matrices for microorganisms and pharmaceuticals.^{22,32}

On the other hand, the disk diffusion test showed that both bacterial strains responded to the TC released from the CNF_TiO₂_TC_M1 sample (Fig. 4(b and d)). The inhibition zones, for both bacterial strains, were similar for CNF_TC_M0 and CNF_TiO₂_TC_M1. However, a trend that the CNF_TC_M0

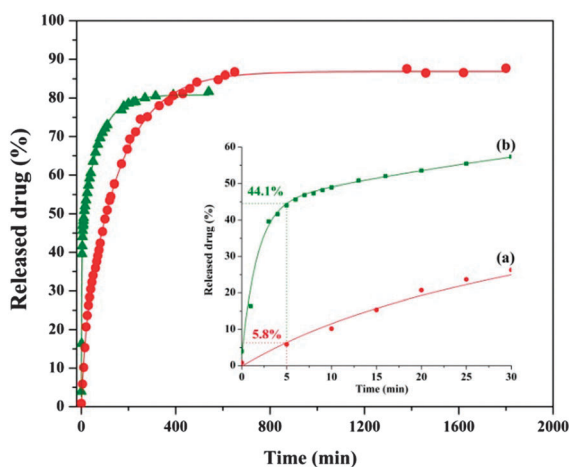


Fig. 3 *In vitro* drug release profiles from the obtained nanocomposites: (a) CNF_TiO₂_TC_M1, (b) CNF_TC_M0.

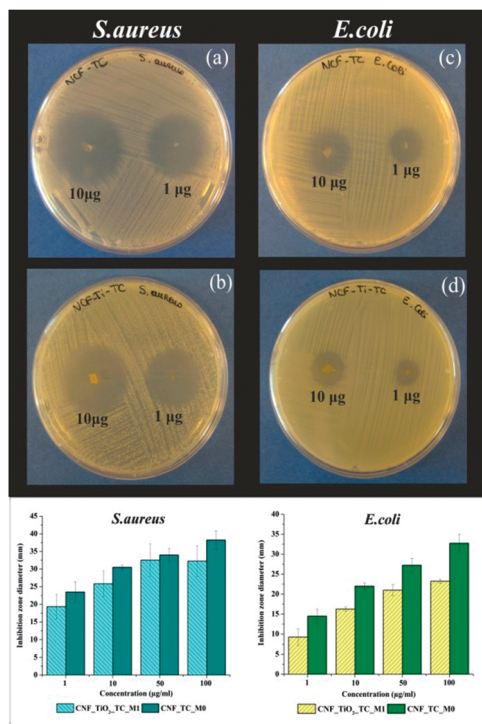


Fig. 4 Visual images of (a and c) CNF_TC_M0 and (b and d) CNF_TiO₂_TC_M1 together with the average inhibition zone.

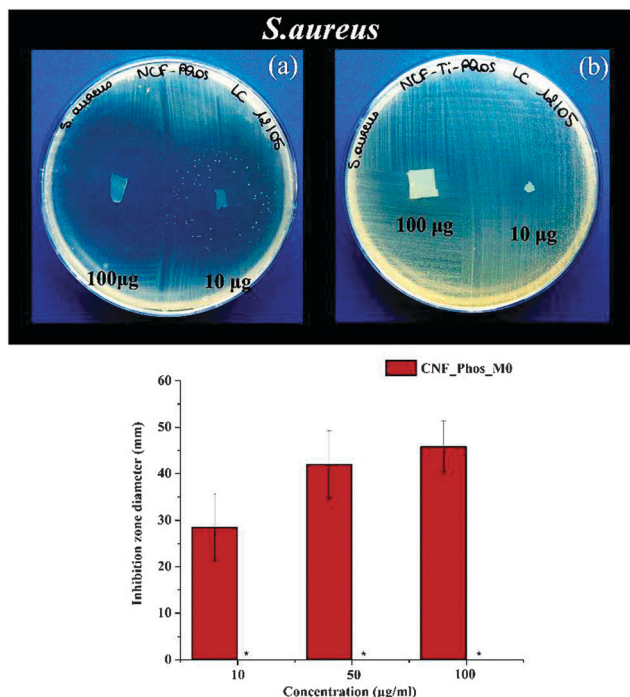


Fig. 5 Visual images of (a) CNF_Phos_M0 and (b) CNF_TiO₂_Phos_M2 together with the average inhibition zone against *S. aureus*; (*) no inhibition zone for CNF_TiO₂_Phos_M2.

sample without titania resulted in a higher inhibition zone was observed, especially for *E. coli* (Table S1 in ESI[†]). Furthermore, as the concentration of TC increased from 10 to 100 µg per disk,

the inhibition zone against *S. aureus* did not dramatically increase for the CNF_TiO₂_TC_M1 sample. Possible explanation for this observation can be attributed to the poor solubility of TC and as a result, its limited diffusion in MH agar. Generally, the size dependence of the inhibition zone on the concentration of an antibiotic is non-linear and often displays saturation caused by its limited solubility.³³

In contrast, the too slow release of Phos from nanocomposites with titania (CNF_TiO₂_Phos_M2) did not permit the drug to achieve a concentration high enough to inhibit bacteria growth, rendering the related nanocomposite formulations inactive. Compared to it, the CNF_Phos_M0 sample obtained without using TiO₂ as a binding agent between the biopolymer and Phos showed good antibacterial activity against both bacterial strains (Fig. 5a). These results were in good agreement with release kinetics of ATP studies¹⁷ and clearly demonstrated that the usage of titania provides much slower release of Phos.

The results from the liquid broth assay also demonstrated the effectiveness of TC released from samples in inhibiting bacterial activity (please, see Table S2 in the ESI[†]). Addition of CNF_TiO₂_TC_M1 or CNF_TC_M0 giving a final concentration of TC in the broth 10 µg mL⁻¹, i.e. 10× MIC, simultaneously as bacteria inoculation resulted in complete growth inhibition of *S. aureus*. The same results were revealed when decreasing the concentration of TC to 1 µg mL⁻¹, i.e. the MIC value for *S. aureus*. This implies that all TC molecules loaded on the cellulose nanofibers are released to the media in a bio-active form.

In the view of the long-term release profile of Phos, we further investigated the antibacterial effect of cellulose nanofibers and nanocomposites against *S. aureus* in liquid broth (MH) after delayed inoculation of the bacteria. For this purpose, nanocomposites grafted with Phos were subjected to a time delay of 12, 18 and 24 h at 37 °C before bacteria inoculation. The results from the liquid broth assay are summarized and presented in Table S2 (please, see ESI[†]). Nanocomposites grafted with Phos in concentration of 10× MIC reduced bacterial growth compared to control without cellulose nanofibers (data not shown), but did not result in a complete growth inhibition. This implies that less than 10% of the Phos is released in a bio-active form under these experimental conditions. Not even delaying the bacteria inoculation with 24 h resulted in a complete growth inhibition. On the other hand, complete growth inhibition was found for the CNF_TiO₂_Phos_M2 sample with immediate inoculation of *S. aureus* when citric buffer (0.03 M, pH = 6) was added to the growth media. The same applies for cellulose nanofibers loaded with Phos but without titania. It is important to mention that polycarboxylate ligands such as citrate or lactate are present in the tissues in a high concentration when an inflammation process takes place. In our recent publication, titania nanosol was used for bioencapsulation and subsequent release (biodelivery) of encapsulated cells or drugs where citrate buffer (pH = 6) was applied to achieve the complete dissolution of titania.³² Hence, the citrate buffer was used here as a model for body fluid conditions as well as to dissolve titania otherwise strongly binding to Phos. Consequently, the enhanced speed of drug

release resulted in increased antibacterial activity of CNF_TiO₂-Phos_M2. It is also noteworthy that strong chemical interactions between drug molecules and the nanocomposite may lead to a complete loss of medical properties of drugs.³⁴ Our results showed that in spite of strong binding by intermolecular interactions between these components, the released drug retains its medicinal properties against pathogen microorganism and confirmed that the drug molecule and the nanocomposite are compatible with each other.

Another important observation is that the TC loaded nanocomposites are able to maintain a good antibacterial effect after UV-irradiation (Table 2). It is well known that TC belongs to a class of compounds that are sensitive to light, and it is classified as a phototoxic drug. Several research groups described the photodecomposition products of TC under different reaction conditions.^{35,36} It is important to note that the intermediate products of the photocatalytic process do not present any antibacterial activity.³⁷ In this sense, it was important to investigate the influence of UV-irradiation on the obtained nanocomposites. For this purpose, we tested the photocatalytic activity of pure cellulose nanofibers and the nanocomposite based on cellulose

nanofibers and TiO₂ by examining the reaction of Rhodamine B degradation under the UV irradiation (Fig. 6). The obtained results showed that no decomposition of an organic dye on PCNFs took place (Fig. 6a). As can be seen from Fig. 6(b), a complete degradation of Rhodamine B was observed already after 20 min under UV irradiation for the CNF_TiO₂ nanocomposite. Quantitative evaluation of the photocatalytic activity was carried out with the CNF_TiO₂ discs immersed into Rhodamine B solutions and is summarized in Fig. 7. The reaction was following the first order kinetics with the constant value $k = 0.124 \text{ min}^{-1}$ ($R^2 = 0.9957$) comparable with the highest values observed under analogous concentration and irradiation conditions for the best TiO₂ based photocatalysts reported so far.^{38,39}

Titania nanoparticles, which are used for cellulose nanofibers modification, have a crystalline core covered with an amorphous layer of triethanolamine (see Fig. S3, ESI†). It should be mentioned that despite the observed high photocatalytic properties of the CNF_TiO₂ sample, the initial titania nanosol does not display any noticeable photochemical activity according to the photocatalytic test with Rhodamine B (see Fig. S4, ESI†).³² UV activity of the CNF_TiO₂ sample can be explained by the

Table 2 Antimicrobial activity of samples after UV-irradiation against *S.aureus*

| Sample | Concentration (µg per disk) | Inhibition zone (mm) without UV-irradiation | Inhibition zone (mm) after 30 min of UV-irradiation | Inhibition zone (mm) after 60 min of UV-irradiation |
|-----------------------------|-----------------------------|---|---|---|
| CNF_TC_M0 | 1 | 23.5 ± 2.9 | 13.8 ± 4.0 | 12.3 ± 3.8 |
| | 10 | 30.5 ± 0.6 | 26 ± 1.4 | 23.3 ± 0.5 |
| | 100 | 38.3 ± 2.6 | 33.5 ± 1 | 31.8 ± 1.3 |
| CNF_TiO ₂ _TC_M1 | 1 | 19.3 ± 3.4 | 11.3 ± 1.7 | 10.5 ± 1.7 |
| | 10 | 25.8 ± 3.7 | 27.0 ± 2.1 | 25.5 ± 1.3 |
| | 100 | 32.3 ± 4.4 | 33.2 ± 1.0 | 32.3 ± 1.7 |

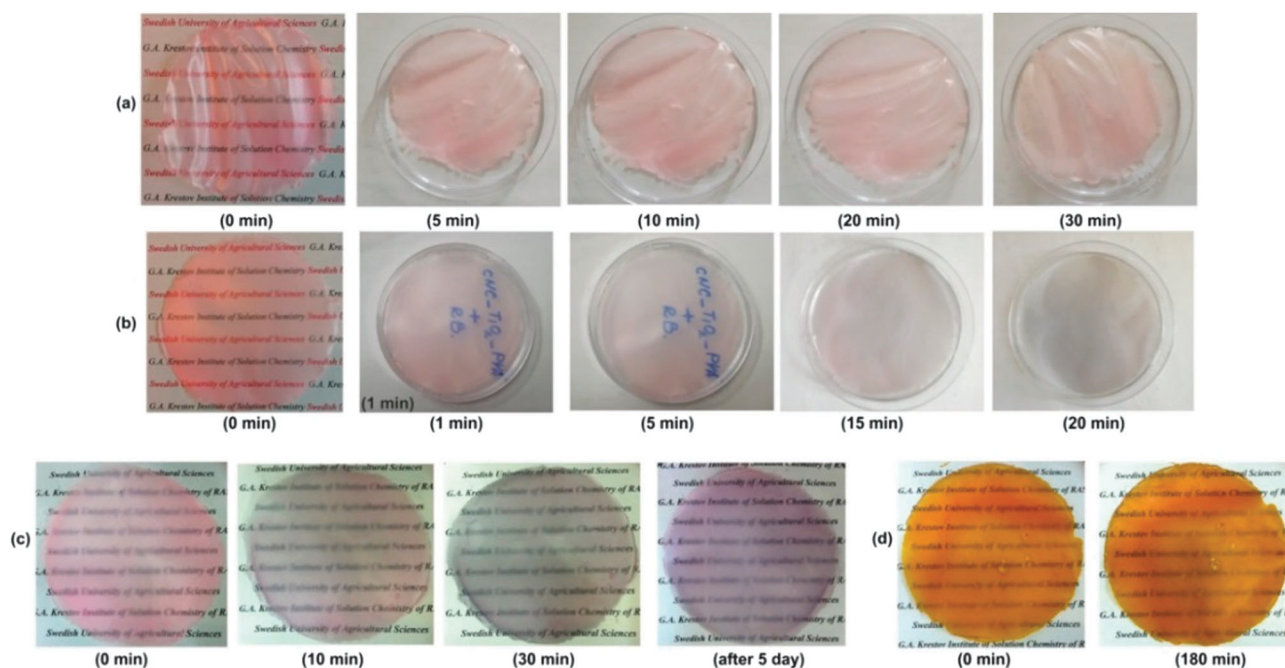


Fig. 6 Photocatalytic activity of (a) PCNFs, (b) CNF_TiO₂, (c) CNF_TiO₂-Phos_M2, (d) CNF_TiO₂-TC_M1 under UV-irradiation.

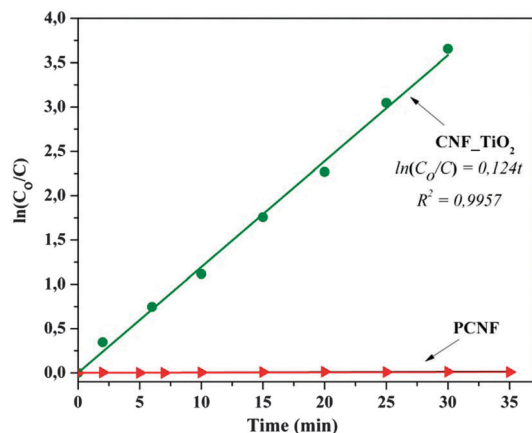


Fig. 7 Kinetics of Rhodamine B degradation (linear transform $\ln(C_0/C)$ vs. t) in photocatalytic experiments using CNF_TiO_2 as a photocatalyst in comparison with PCNFs.

presence of carboxylic groups in the butane-tetracarboxylate linker, which activates the crystalline core of TiO_2 under UV-irradiation. Sensibilization of the titania surface in the presence of polycarboxylate ligands is a well investigated phenomenon. The details of reaction mechanisms have been revealed in the work of Bürgi *et al.*⁴⁰

The photocatalytic properties of nanocomposites modified with TiO_2 and the drugs were found, however, to be completely different in comparison with pure and TiO_2 -modified cellulose nanofibers. Specifically, the $\text{CNF_TiO}_2\text{-TC_M1}$ sample did not display any photocatalytic activity (Fig. 6d). Decomposition of Rhodamine B did not occur even after 3 hours of UV irradiation. A possible explanation for this effect is that the complexation of the titania with the extended aromatic system of the TC drug results in a system acting as a trap, causing immediate recombination of the electron-hole pairs created by irradiation. The discovered localization of the Ti^{3+} sites in the case of Phos derived materials (please, see below) provided an indirect confirmation to this supposition.

The nanotitania in this case acts as protection of TC against UV-rays. It should be mentioned that a large number of studies are focused on the removal of TC-related compounds by UV-irradiation. In particular, several research groups described the effects of titania on the kinetics and mechanism of photo degradation of TC.^{37,41–44} The titania used in these literature studies consisted of much bigger fully crystalline particles and possessed much lower active surface area. Apparently, its activity in contrast to that in our case could not be quenched by surface complexation with TC.

In the view that TC as effective broad-spectrum antibiotic is widely used for wound healing, its protection against UV-rays is also a very important goal in the development of antibacterial patches. The results of the disk diffusion tests of $\text{CNF_TiO}_2\text{-TC_M1}$ confirmed that the released TC retains its medicinal properties without decreasing of any biological activity after 30 and 60 min of UV treatment against *S. aureus* (Table 2). No colour change is observed for this sample under UV irradiation (see Fig. 6d).

In the case of a CNF_TC_M0 sample obtained without using titania as a binding agent, a significant drop of antibacterial activity was observed.

In the case of Phos, $\text{CNF_TiO}_2\text{-Phos_M2}$ displayed a photochromic effect, *i.e.* colour change from pink to purple under UV-light for 10 min (Fig. 6c). More interestingly, the purple colour slowly returned to pink within 5 days following the end of the UV exposure. We suggested that this change in colour can be attributed to the transition of Ti^{4+} to Ti^{3+} under UV-irradiation and the following formation of the complexes with the drug molecule.⁴⁵ Moreover, the reverse transition of colour shows that the formed complexes are not redox stable and are re-oxidized over time. The proposed mechanism could be confirmed by EPR studies (see Fig. 8). The nano cellulose matrices themselves (PCNFs, *i.e.* wet gel of $\text{CNF_TiO}_2\text{-Phos_M2}$) did not display any distinct EPR signals (Fig. 8, green spectrum). In contrast, the wet gel of $\text{CNF_TiO}_2\text{-Phos_M2}$ freshly exposed to UV for 5 min displayed a distinct EPR signal (Fig. 8, blue). This spectrum could be assigned to originate from Ti^{3+} centers as a result of the reduction of TiO_2 after UV-irradiation.^{46,47} A similar but narrower signal was observed in the sample stored for 5 days after light exposure, displaying a much weaker signal intensity (see Fig. 8 blue and red spectra). The broader and stronger spectrum from the sample after short light exposure reflects the intactness of the matrices whereas the less intensity and narrowing of the signal may be attributed to the decay of Ti^{3+} and at least partial desorption of the Phos ligands. The latter resulted in a simplified coordination arrangement of the paramagnetic sites.^{48,49}

There is growing interest in the development of nanocomposites based on biopolymers for biomedical applications. In our present work we describe the production of a new type of dermal drug delivery system based on cellulose nanofibers and titania nanoparticles with chemically immobilized drugs. We demonstrated different antibacterial activities of the two different types of

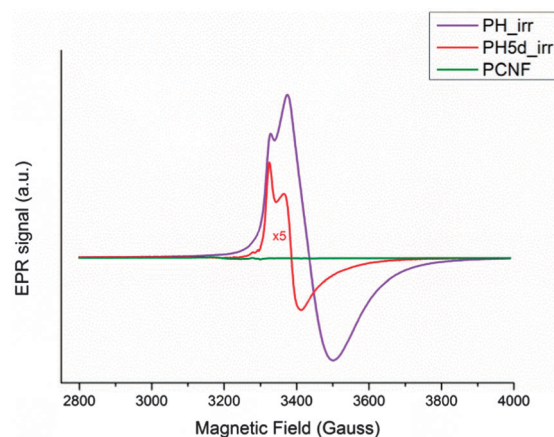


Fig. 8 EPR spectra of PCNFs (green), wet gel produced according to the $\text{CNF_TiO}_2\text{-Phos_M2}$ method; PH_irr (blue), UV irradiated for 5 min using a 250 W lamp and PH5d_irr (red), the same treatment as in PH_irr but stored for 5 days after irradiation (note that this spectrum is magnified 5 times for easy comparison). EPR recording settings: microwave frequency 9.29 GHz; power 20 μW ; modulation frequency 100 kHz; amplitude 10 G; $T = 7$ K.

antibiotic drugs TC and Phos immobilized into the nanocomposites. These results can be explained by differences in their binding to nanocomposites, which influence the speed of the drug release and thus determine the possibility of achieving the minimal concentration required for bacterial growth inhibition. It has already been shown that titania nanoparticles have a strong affinity for phosphorylated ligands.²² The results of the *in vitro* microbiological tests are in good agreement with the observed rendered bioactivity. At the same time, the long-term release from these nanocomposites may find application for disinfectants with prolonged action to avoid bacterial growth. On the other hand, the relatively weaker phenoxide binding between TC and modified biopolymers makes possible the use of these nanocomposites as efficient antibacterial patches against pathogenic bacteria even under UV exposure.

Conclusions

In vitro antibacterial activity of two antibiotics drugs, TC and Phos, loaded to nanocomposites based on cellulose nanofibers and titania nanoparticles against two potential pathogens, *S. aureus* and *E. coli*, was investigated. The results of bacterial susceptibility tests showed that both released drugs retained their medicinal properties against bacteria. However, due to the long-term release profile of Phos, an antibacterial activity of nanocomposites modified with Phos was observed only after the addition of citrate buffer. Nanocomposites modified with TC were also found to maintain their antibacterial properties after 60 minutes of UV treatment.

In addition, the photocatalytic test also showed that nanocomposites based on cellulose nanofibers and modified only with titania nanoparticles possess high photocatalytic properties and can be utilized in photovoltaic devices and photocatalysis.

This new drug delivery system, based on nanocellulose and titania which can be loaded with different classes of medicines, can potentially be used within various therapeutic applications.

Acknowledgements

The authors would like to express their gratitude to the Swedish Research Council (Vetenskapsrådet) for the support of the projects "Molecular precursors and molecular models of nano-porous materials" and "Basic research driving the development of solar fuels" and to Knut and Alice Wallenbergs Foundation (P.H.). O. Galkina would like to thank the Swedish Institute for a PhD scholarship.

The authors express their gratitude to Prof. Stenbjörn Styring and to Dr. Anders Thapper for valuable discussions.

References

- 1 K. Moodley, V. Pillay, Y. E. Choonara, L. C. du Toit, V. M. Ndesendo, P. Kumar, S. Cooppan and P. Bawa, *Int. J. Mol. Sci.*, 2012, **13**, 18.
- 2 E. Merisko-Liversidge and G. G. Liversidge, *Adv. Drug Delivery Rev.*, 2011, **63**, 427.
- 3 J. Xu, S. Strandman, J. X. Zhu, J. Barralet and M. Cerruti, *Biomaterials*, 2015, **37**, 395.
- 4 M. Hittinger, J. Juntke, S. Kletting, N. Schneider-Daum, C. de Souza Carvalho and C. M. Lehr, *Adv. Drug Delivery Rev.*, 2015, **85**, 44.
- 5 S. Moritz, C. Wiegand, F. Wesarg, N. Hessler, F. A. Müller, D. Kralisch, U. C. Hipler and D. Fischer, *Int. J. Pharm.*, 2014, **471**, 45.
- 6 A. Schroeter, T. Engelbrecht, R. H. Neubert and A. S. Goebel, *J. Biomed. Nanotechnol.*, 2010, **6**, 511.
- 7 E. Touitou, B. Godin and C. Weiss, *Drug Dev. Res.*, 2000, **50**, 406.
- 8 P. Wu and D. W. Grainger, *Biomaterials*, 2006, **27**, 2450.
- 9 N. D. Stebbins, M. A. Ouimet and K. E. Uhrich, *Adv. Drug Delivery Rev.*, 2014, **78**, 77.
- 10 J. J. Escobar-Chávez, R. Díaz-Torres, I. M. Rodríguez-Cruz, C. L. Domínguez-Delgado, R. Sampere Morales, E. Ángeles-Anguiano and L. M. Melgoza-Contreras, *Res. Rep. Transdermal Drug Delivery*, 2012, **1**, 3.
- 11 N. Barkalina, C. Charalambous, C. Jones and K. Coward, *Nanomedicine*, 2014, **10**, 921.
- 12 R. C. Rowe, P. J. Sheskey and S. C. Owen, *Handbook of Pharmaceutical Excipients*, Pharmaceutical Press, American Pharmacists Association, Washington, 5th edn, 2006.
- 13 R. Kolakovic, L. Peltonen, A. Laukkanen, M. Hellman, P. Laaksonen, M. B. Linder, J. Hirvonen and T. Laaksonen, *Eur. J. Pharm. Biopharm.*, 2013, **85**, 1238.
- 14 K. Missoum, M. N. Belgacem and J. Bras, *Materials*, 2013, **6**, 1745.
- 15 N. Lin and A. Dufresne, *Eur. Polym. J.*, 2014, **59**, 302.
- 16 E. M. Fernandes, R. A. Piresa, J. F. Manoa and R. L. Reisa, *Prog. Polym. Sci.*, 2013, **38**, 1415.
- 17 O. L. Galkina, V. K. Ivanov, A. V. Agafonov, G. A. Seisenbaeva and V. G. Kessler, *J. Mater. Chem. B*, 2015, **3**, 1688.
- 18 European Committee of Antimicrobial Susceptibility Testing. Disk diffusion method, 2014, <http://www.eucast.org>, EUCAST Version 4.0.
- 19 C. Q. Yang, *Text. Res. J.*, 2001, **71**, 201.
- 20 V. A. Dehabadi, H. J. Buschmann and J. S. Gutmann, *Text. Res. J.*, 2013, **83**, 1974.
- 21 R. Pazik, R. Andersson, L. Kepinski, J. M. Nedelec, V. G. Kessler and G. A. Seisenbaeva, *J. Phys. Chem. C*, 2011, **115**, 9850.
- 22 G. A. Seisenbaeva, M. P. Moloney, R. Tekoriute, A. Hardy-Dessources, J. M. Nedelec, Y. K. Gun'ko and V. G. Kessler, *Langmuir*, 2010, **26**, 9809.
- 23 A. Castaneda-Garcia, J. Blazquez and A. Rodriguez-Rojas, *Antibiotics*, 2013, **2**, 217.
- 24 M. Shavit, D. Peri, C. M. Manna, J. S. Alexander and E. Y. Tshuva, *J. Am. Chem. Soc.*, 2007, **129**, 12098.
- 25 B. Malisova, S. Tosatti, M. Textor, K. Gademann and S. Zürcher, *Langmuir*, 2010, **26**, 4018.
- 26 P. Karuppuswamy, J. R. Venugopal, B. Navaneethan, A. L. Laiva and S. Ramakrishna, *Mater. Lett.*, 2015, **141**, 180.
- 27 WHO Model List of Essential Medicines. World Health Organization, http://apps.who.int/iris/bitstream/10665/93142/1/EML_18_eng.pdf?ua=;2014, accessed April 2014.

- 28 O. L. Galkina, A. Sycheva, A. Blagodatskiy, G. Kaptay, V. L. Katanaev, G. A. Seisenbaeva, V. G. Kessler and A. V. Agafonov, *Surf. Coat. Technol.*, 2014, **253**, 171.
- 29 H. M. Myers, H. J. Tochon-Danguy and C. A. Baud, *Calcif. Tissue Int.*, 1983, **35**, 745.
- 30 J. S. Boateng, K. H. Matthews, H. N. Stevens and G. M. Eccleston, *J. Pharm. Sci.*, 2008, **97**, 2892.
- 31 J. Hurler, O. A. Berg, M. Skar, A. H. Conradi, P. J. Johnsen and N. Skalko-Basnet, *J. Pharm. Sci.*, 2012, **101**, 3906.
- 32 V. G. Kessler, G. A. Seisenbaeva, M. Unell and S. Hakansson, *Angew. Chem., Int. Ed.*, 2008, **47**, 8506.
- 33 J. Kim, M. R. Marshall and C. Wei, *J. Agric. Food Chem.*, 1995, **43**, 2839.
- 34 N. D. Burkhanova, S. M. Yugai, S. S. Khalikov, M. M. Turganov and G. V. Nikonovich, Kh. N. Aripov, *Chem. Nat. Compd.*, 1997, **33**, 340.
- 35 A. Eremenko, N. Smirnova, I. Gnatiuk, O. Linnik, N. Vityuk, Y. Mukha and A. Korduban, in *Nanocomposites and Polymers with Analytical Methods*, ed. J. Cuppoletti, InTech, Croatia, 2011, ch. 3, pp. 51–83.
- 36 W. H. K. Sanniez and N. Pilpel, *J. Pharm. Sci.*, 1980, **69**, 5.
- 37 C. Reyes, J. Fernández, J. Freer, M. A. Mondaca, C. Zaror, S. Malato and H. D. Mansilla, *J. Photochem. Photobiol., A*, 2006, **184**, 141.
- 38 J. C. Zhao, T. X. Wu, K. Q. Wu, K. Oikawa, H. Hidaka and N. Seprone, *Environ. Sci. Technol.*, 1998, **32**, 2394.
- 39 Y. J. Li, S. G. Sun, M. Y. Ma, Y. Z. Ouyang and W. B. Yan, *Chem. Eng. J.*, 2008, **142**, 147.
- 40 I. Dolamic and T. Bürgi, *J. Catal.*, 2007, **248**, 268.
- 41 A. Di Paola, M. Addamo, V. Augugliaro, E. García-López, V. Loddo, G. Marci and L. Palmisano, *Fresenius Environ. Bull.*, 2004, **13**, 1275.
- 42 M. Addamo, V. Augugliardo, A. Di Paola, E. García-López, V. Loddo, G. Marci and L. Palmisano, *J. Appl. Electrochem.*, 2005, **35**, 765.
- 43 Y. Liu, X. Gan, B. Zhou, B. Xiong, J. Li, C. Dong, J. Bai and W. Cai, *J. Hazard. Mater.*, 2009, **171**, 678.
- 44 Y. Chen, C. Hu, J. Qu and M. Yang, *J. Photochem. Photobiol., A*, 2008, **197**, 81.
- 45 C. Sanchez, L. Rozes, F. Ribot, C. Laberty-Robert, D. Grosso, C. Sassoie, C. Boissiere and L. Nicole, *C. R. Chim.*, 2010, **13**, 3.
- 46 P. Lombard, N. Ollier and B. Boizot, *J. Non-Cryst. Solids*, 2011, **357**, 1685.
- 47 S. Van Doorslaer, C. Di Valentin and G. Paccioni, *Inorg. Chem.*, 2011, **50**, 2385.
- 48 A. A. Minnekhanov, D. M. Deygen, E. A. Konstantinova, A. S. Vorontsov and P. K. Kashkarov, *Nanoscale Res. Lett.*, 2012, **7**, 333.
- 49 B. C. Qiu, Y. Zhou, Y. F. Ma, X. L. Yang, W. Q. Sheng, M. Y. Xing and J. L. Zhang, *Sci. Rep.*, 2015, **5**, 8591.